Phosphatidylinositol-3-Kinase/Akt Regulates Bleomycin-Induced Fibroblast Proliferation and Collagen Production

Yongju Lu[1]*, Neelam Azad[2]*, Liying Wang[3], Anand K. V. Iyer[1], Vincent Castranova[3], Bing-Hua Jiang[4], and Yon Rojanasakul[1,4]

[1]Department of Pharmaceutical Sciences and [4]Mary Babb Randolph Cancer Center, West Virginia University, Morgantown, West Virginia; [2]Department of Pharmaceutical Sciences, Hampton University, Hampton, Virginia; and [3]Pathology and Physiology Research Branch, National Institute For Occupational Safety and Health, Morgantown, West Virginia

Abnormal repair and dysregulated angiogenesis have been implicated in the pathogenesis of pulmonary fibrosis, but the underlying mechanisms of regulation are not well understood. The present study investigated the role of phosphatidylinositol-3-kinase (PI3K)/Akt in fibrogenesis of human lung fibroblasts and its regulation by reactive oxygen species (ROS). Exposure of lung fibroblasts to bleomycin, a known inducer of fibrosis, resulted in rapid activation of PI3K/Akt and a parallel increase in fibroblast proliferation and collagen production, characteristics of lung fibrosis. Bleomycin had no significant effect on total Akt protein expression but induced phosphorylation of the protein at threonine 308 and serine 473 positions. Inhibition of this phosphorylation by PI3K inhibitors or by dominant-negative Akt (T308A/S473A) expression abrogated the effects of bleomycin on fibroblast proliferation and collagen production, suggesting the role of PI3K/Akt in the fibrogenic process. Activation of PI3K/Akt by bleomycin also led to transcriptional activation and protein expression of hypoxia-inducible factor-1α (HIF-1α) and vascular endothelial growth factor, which contributed to the fibroproliferative and collagen-inducing effects of bleomycin. The fibrogenic effects of bleomycin were dependent on ROS generation, particularly superoxide anion and hydrogen peroxide, which were induced by bleomycin. Inhibition of ROS generation by antioxidant enzymes, catalase and superoxide dismutase mimetic MnTBAP, abrogated the fibrogenic effects of bleomycin as well as its induction of PI3K/Akt and HIF-1α activation. Together, our results indicate a novel role of PI3K/Akt in fibrogenesis of human lung fibroblasts and its regulation by ROS, which could be exploited for the treatment of pulmonary fibrosis and related disorders.

Keywords: collagen; bleomycin; PI3K; Akt; ROS

CLINICAL RELEVANCE

This study suggests that in addition to its normal role as an angiogenesis regulator, the PI3K/Akt also serves as a key regulator of fibrogenesis by inducing fibroblast cell proliferation and collagen synthesis via a redox-dependent mechanism. These data have important implications in the design of more effective strategies for the treatment of pulmonary fibrosis and related disorders.

Pulmonary fibrosis is a progressive and lethal lung disease characterized by excessive proliferation of fibroblasts and deposition of extracellular matrix (ECM) (1, 2). The most common form of pulmonary fibrosis is idiopathic pulmonary fibrosis, which has a prevalence rate of 14 to 43 cases per 100,000 persons (3). Life expectancy after diagnosis of the disease varies, but is on average less than 5 years (4). Despite improvements in the diagnostic approach to pulmonary fibrosis and active research in recent years, the molecular mechanisms of the disease remain poorly understood and effective drug therapy has yet to be developed (5, 6). It has been widely held that chronic inflammation injures the lung and modulates fibrogenesis, leading to the end-stage fibrotic scar. However, therapeutic strategies based on the use of anti-inflammatory and immunosuppressive agents are not effective in treating the disease (6). Furthermore, increasing evidence suggests that fibroblast proliferation, and not chronic inflammation, constitutes the primary events of ongoing lung injury and activation associated with evolving fibrosis (7, 8). Mortality is increased in patients with pulmonary fibrosis with greater profusion of fibroblastic foci on lung histopathology (9, 10), suggesting that the activation and persistence of fibroblasts may be a critical regulatory event in the pathogenesis of pulmonary fibrosis. Recent studies also suggest that fibrogenesis is associated with abnormal repair and dysregulated angiogenesis (11, 12). Elaboration of a provisional ECM by fibroblasts is an early repair function that aids epithelial cell migration and regeneration to restore barrier functions and maintain tissue architecture (13). Studies in both animal models and tissue specimens from patients with pulmonary fibrosis showed an abnormal repair and exaggerated angiogenesis. However, the mechanism underlying this process and its effect on lung fibrogenesis are unclear.

Since angiogenesis is known to be regulated by PI3K/Akt and since the role of this pathway in fibrogenesis is not well understood, we sought to determine its role and elucidate the underlying mechanism of regulation. We hypothesized that PI3K/Akt plays a role in fibrogenesis in part through its activation of fibroblast cell proliferation and production of collagen matrix. The PI3K/Akt pathway is involved in many cellular processes, including cell growth, differentiation, apoptosis, and angiogenesis (14, 15), and is commonly triggered by the activation of receptor tyrosine kinases, which leads to the translocation of PI3K from cytoplasm to plasma membrane. This translocation activates its catalytic subunit (p110α), which in turn induces phosphorylation of phosphoinositides, leading to the formation of second messengers (PI3, 4-biphosphate and PI3, 4,5-triphosphate) that bind to the pleckstrin-homology domain of Akt (16, 17). This binding induces a conformational

(*Received in original form January 5, 2009 and in final form May 18, 2009*)

This work was supported by National Institutes of Health Grant R01HL76340.

* These two authors contributed equally to this work.

Disclaimer: The findings and conclusions in this report are those of the authors and do not necessarily represent the views of the National Institute for Occupational Safety and Health.

Correspondence and requests for reprints should be addressed to Yon Rojanasakul, Ph.D., West Virginia University, Department of Pharmaceutical Sciences, P.O. Box 9530, Morgantown, WV 26506. E-mail address: yrojan@hsc.wvu.edu

Am J Respir Cell Mol Biol Vol 42. pp 432–441, 2010
Originally Published in Press as DOI: 10.1165/rcmb.2009-0002OC on June 11, 2009
Internet address: www.atsjournals.org

change of Akt that exposes two amino acid residues, serine 473 and threonine 308, which are phosphorylated by PDK1 and PDK2, respectively. The phosphorylation of these two amino acids is necessary for Akt activation, which induces downstream signaling molecules leading to various cellular functions. Previous studies indicate that PI3K/Akt is a key signaling pathway involved in the activation of hypoxia-inducible factor-1 (HIF-1) (18–21). HIF-1 is a heterodimer composed of HIF-1α and HIF-1β subunits. HIF-1α is a unique subunit that is induced in response to various stimuli, including hypoxia, cytokines, and growth factors, through redox regulation (22–24). HIF-1β is identical to the aryl hydrocarbon nuclear translocator (25, 26) and is not regulated by cellular redox state (27). HIF-1 regulates the expression of various target genes. One of the most important genes regulated by HIF-1 is vascular endothelial growth factor (VEGF) (28–30).

VEGF is abnormally regulated in patients with fibrotic diseases, including idiopathic myelofibrosis (12) and diffuse lung fibrosis (31), and in an animal model of bleomycin-induced lung fibrosis (32). Since VEGF is a key target of PI3K/Akt signaling pathway (22, 33, 34), these studies suggest an involvement of the PI3K/Akt pathway in fibrogenesis. However, direct evidence for the role of PI3K/Akt in the fibrotic process is still lacking. Furthermore, the mechanism by which PI3K/Akt is regulated during this process is unclear. To allow mechanistic investigations of the role of PI3K/Akt in this process, we used genetic and pharmacologic approaches to modulate PI3K/Akt and studied its effect on fibrogenesis of lung fibroblasts by examining their proliferative and collagen-producing activities in response to bleomycin treatment. We showed that activation of PI3K/Akt is critically involved in the fibroproliferative and collagen-inducing effects of bleomycin, and that these effects are mediated in part through HIF-1α→VEGF signaling pathway. The induction of fibrogenic signaling pathway was also shown to be dependent on ROS generation, particularly superoxide anion and hydrogen peroxide, thus revealing a novel mechanism of fibrogenesis regulation that could have important implications in antifibrotic therapy.

MATERIALS AND METHODS

Reagents and Cell Culture

Antibodies against Akt and phospho-Akt Ser473 and Thr308 were obtained from Cell Signaling Technology, Inc. (Beverly, MA). Antibodies for collagen type I and type III were from Fitzgerald (Concord, MA). Antibodies for HIF-1α, β-actin, and horseradish peroxidase (HRP)-conjugated secondary antibodies were from Santa Cruz Biotechnology (Santa Cruz, CA). Human VEGF immunoassay kit, a neutralizing antibody against VEGF, and its nonspecific control antibody were from R&D Systems (Minneapolis, MN). LY-294002, wortmannin, PD98059, and Mn(III) tetrakis (4-benzoic acid) porphyrin (MnTBAP) were obtained from Calbiochem (La Jolla, CA). Catalase was from Roche Molecular Biochemicals (Indianapolis, IN). Akt mutant plasmid (SRα-Akt T308A/S473A) and control plasmid were a gift from C. Huang (New York University, Tuxedo, NY). VEGF reporter (VEGF-luc) and control plasmid were obtained from American Type Culture Collection (ATCC, Manassas, VA). All other chemicals and reagents including bleomycin sulfate, dihydroethidine, and dichlorofluorescein diacetate were from Sigma Chemical, Inc. (St. Louis, MO).

The human lung fibroblast CRL-1490 cell line was obtained from ATCC. The cells were maintained in Eagle's Minimum Essential medium (MEM) supplemented with 10% fetal bovine serum (FBS), 100 U/ml penicillin, and 100 μg/ml streptomycin. They were cultured at 37°C in 5% CO_2 incubator. The cells were passaged at preconfluent densities using a solution containing 0.05% trypsin and 0.5 mM EDTA.

Cell Proliferation and Collagen Assays

Cells were seeded in 12-well plates at a density of 2×10^5 cells/well in MEM supplemented with 10% FBS at 37°C in a 5% CO_2 incubator. At various times after the treatment, cells were scraped and washed twice with phosphate-buffered saline (PBS) and centrifuged at 1,000 × *g* for 5 minutes. Cells were resuspended in 1 ml of Hanks' balanced salt solution and counted using a hemocytometer. A minimum of three separate experiments was performed for each assay. Collagen content was determined by Western blotting as described below and by Sircol assay (Biocolor Ltd, Belfast, UK), according to the manufacturer's protocol. Briefly, Sirius red reagent (50 μl) was added to cell culture supernatant (50 μl) and mixed for 30 minutes. The collagen–dye complex was precipitated by centrifugation at 16,000 × *g* for 5 minutes, washed with ethanol, and dissolved in 0.5 M NaOH. The samples were introduced into a microplate reader and read for absorbance at 540 nm.

Apoptosis Assay

Apoptosis was determined using an enzyme-linked immunosorbent assay (ELISA)-based DNA fragmentation assay kit (Roche Molecular Biochem., Indianapolis, IN), according to the manufacturer's instructions. Briefly, cells were lysed with 200 μl of lysis buffer at room temperature, and the cell lysate (20 μl) was mixed with an antibody solution (80 μl) at room temperature for 2 hours. The substrate was then added after the wells were washed three times with a washing buffer. After incubation for 15 minutes at 37°C, optical density was measured using a microplate reader at the wavelength of 405 nm.

Western Blot Analysis

After specific treatments, cells were harvested and lysed on ice for 30 minutes in lysis buffer containing 150 mM NaCl, 100 mM Tris (pH 8.0), 1% Triton X-100, 1% deoxycholic acid, 0.1% SDS, 5 mM EDTA, 10 mM sodium formate, 1 mM sodium orthovanadate, 2 mM leupeptin, 2 mM aprotinin, 1 mM phenylmethylsulfonyl fluoride, 1 mM dithiothreitol, and 2 mM pepstatin A. After centrifugation at 14,000 × *g* for 15 minutes at 4°C, the supernatant was collected as the total cellular protein extract. The protein concentrations were determined using a bicinchoninic acid protein assay kit (Pierce Biotechnology, Rockford, IL). Equal amount of proteins per sample (20 μg) were resolved on a 10% sodium dodecyl sulfate-polyacrylamide gel electrophoresis (SDS-PAGE) and transferred onto a nitrocellulose membrane. The membrane was blocked with T-PBS (0.3% Tween-20 in PBS) containing 3% dry milk and incubated with primary antibody overnight at 4°C. After three washes with T-PBS, the membrane was incubated with HRP-conjugated secondary antibody for 1 hour and then washed with 0.05% Tween-20 in PBS. Immunoreactive proteins were detected by chemiluminescence (Supersignal West Pico; Pierce, Rockford, IL) and quantified by imaging densitometry using UN-SCAN-IT digitizing software (Silk Scientific, Orem, UT). Mean densitometry data from independent experiments were normalized to results in cells from control experiments.

ROS Detection

Cellular ROS production was determined fluorometrically using dihydroethidine (DHE) and dichlorofluorescein diacetate (DCF-DA) as fluorescent probes for superoxide and peroxide, respectively. After specific treatments, cells were incubated with the probes (10 μM) for 30 minutes at 37°C, after which they were washed, resuspended in PBS, and analyzed for fluorescence intensity using a multiwell plate reader (FLUOstar OPTIMA; BMG LABTECH Inc., Durham, NC) at the excitation/emission wavelengths of 485/535 nm and 485/610 nm for DHE and DCF fluorescence measurements, respectively.

Stable Transfection of Dominant-Negative Akt

CRL-1490 cells were cultured in a 6-well plate until they reached 70 to 80% confluence. The cells were transfected with 1 μg of CMV-neo vector and 15 μl of Lipofectamine 2000 (Invitrogen, Carlsbad, CA) along with 2 μg of mutated Akt (SRα-Akt T308A/S473A) or control plasmid in the absence of serum. After 5 hours, the medium was replaced with 5% FBS MEM, and 36 hours later they were trypsinized and plated onto 75-ml culture flasks. The cells were then cultured in G418 selection medium (400 μg/ml) for 28 days. The selected cells were grown in G418-free MEM for two passages before each experiment.

VEGF Protein and Reporter Gene Assays

For analysis of VEGF protein, cells were plated in a 6-well plate at a density of 2×10^5 cells/well in culture medium and incubated overnight

before the cells were subjected to treatment. After the treatment, cell supernatants were collected and analyzed for VEGF protein levels using a Quantikine ELISA kit (R&D Systems). Cell samples or reference standards (200 μl) were added to the wells of a microplate that was precoated with a monoclonal antibody specific to VEGF and incubated for 2 hours at room temperature. After washing unbounded substances, an HRP-conjugated polyclonal antibody against VEGF was added to the wells and incubated for 2 hours at room temperature. After washing and addition of 200 μl of substrate solution, optical density was determined on a microplate reader at 450 nm.

For *VEGF* reporter gene assay, cells were seeded in 12-well plates and cultured to 50 to 60% confluence. Cells were transfected with 1 μg of either *VEGF* reporter (VEGF-luc) plasmid (ATCC) or control plasmid and 10 ng of pRL-tk normalizing luciferase plasmid (Promega, Madison, WI) using Lipofectamine 2,000 transfecting agent (Invitrogen), according to the manufacturer's protocol. After a 24-hour recovery period, transfected cells were treated with bleomycin for 12 hours and cell extracts were prepared and analyzed for luciferase activity using a Promega dual-luciferase assay kit (Promega). Both firefly and Renilla luciferase activities were measured using a multiwell plate luminometer (BMG LABTECH). Normalized reporter activity was expressed as the firefly luciferase value divided by the Renilla luciferase value. Relative fold activity was calculated as the normalized reporter activity of the treated sample over control.

Reverse Transcription PCR

Total RNA was extracted with TRIZOL (Invitrogen) and reverse transcription PCR was performed with Access RT-PCR System (Promega) according to the manufacturer's instructions. The thermal profiles consisted of 94°C for 3 minutes for initial denaturing followed by 30 cycles of 95°C for 1 minute, 64°C for 1 minute, and 72°C for 1 minute. Specific primers used for PCR are as follows: VEGF (forward, 5′-TCTTCAAGCCATCCTGTGTGC-3′; reverse, 5′-CACATTTGTT GTGCTGTAGGA AGC-3′), HIF-1α (forward, 5′-TGTAATGCTCC CCTCACCCAACGAA-3′; reverse, 5′-CAGGGC TTGCGGAACT GCTTTCTA A-3′), and glyceraldehyde-3-phosphate dehydrogenase (forward, 5′-CGGAGTCAACGGATTTGGTCGTAT-3′; reverse, 5′-AGCCTTCTCCATGGTTGGTGAAGAC-3′). The PCR products were electrophoresed in a 1.5% agarose gel, stained with ethidium bromide, and photographed.

Inhibition of HIF-1α by RNA Interference

Lentiviral transduction particles carrying short hairpin RNA (shRNA sequence against human HIF-1α (5′-CCGGCGGCGAAGTAAAGAAT CTGAACTCGAGTTCAGATTCTTTACTTCGCC GTTTTT-3′) and control non-target sequence (5′-CCGGCAACAAGATGAAGAGC ACCAACTC GAGTTGGTGCTCTTCATCTTGTTGTTTTT-3′) were used to knockdown HIF-1α expression in CRL-1490 cells. The viral vectors were obtained commercially from Sigma Chemical, Inc. (Cat # SHVRS-NM_001530 and SHC002V, respectively) and were used according to the manufacturer's instructions. Briefly, cells were seeded in 6-well plates (5×10^5/well) and incubated with HIF-1α shRNA lentiviral particles or control particles at the multiplicity of infection (MOI) of 1.5 in the presence of hexadimethrine bromide (8 μg/ml) for 36 hours. Transfected cells were analyzed for HIF-1α by Western blotting before use.

Statistical Analysis

The data represent mean ± SD from three or more independent experiments. Statistical analysis was performed by ANOVA and Duncan's comparison tests were used to evaluate the significance between measurements at a significance level of $P < 0.05$.

RESULTS

Bleomycin Induces Fibroblast Proliferation and Collagen Production

To determine whether bleomycin can directly induce fibroblast proliferation and collagen production, human lung fibroblast CRL-1490 cells were treated with various concentrations of bleomycin, and cell growth and collagen protein expression were determined by cytometry and Western blotting, respectively. As shown in Figure 1A, fibroblast proliferation was induced by bleomycin in a dose-dependent manner. The

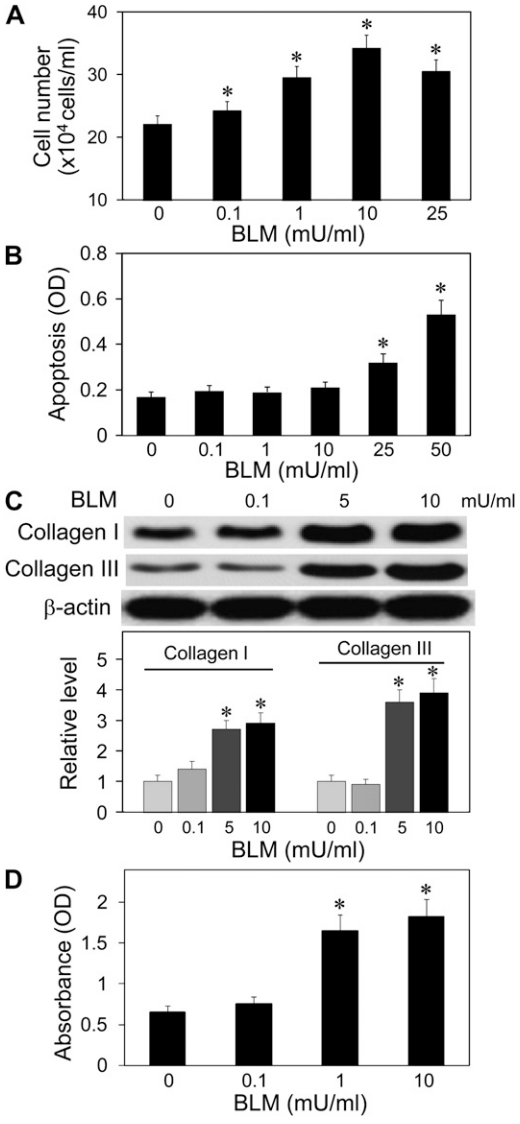

Figure 1. Induction of fibroblast proliferation and collagen production by bleomycin. (*A*) Subconfluent cultures of human lung fibroblast CRL-1490 cells were exposed to various concentrations of bleomycin (0–25 mU/ml) and analyzed for cell growth after 24 hours. (*B*) Cells were similarly exposed to bleomycin for 24 hours and analyzed for apoptosis by enzyme-linked immunosorbent assay (ELISA)-based DNA fragmentation assay. (*C*) Western blot analysis of collagen protein expression in response to bleomycin treatment. Cells were treated with the indicated concentrations of bleomycin for 12 hours, after which they were washed with ice-cold phosphate-buffered saline (PBS) and extracted with SDS sample buffer. The cell extracts were separated on polyacrylamide-SDS gels, transferred, and probed with antibodies specific for human collagen type I and III. Blots were reprobed with β-actin antibody to confirm equal loading of the samples. The immunoblot signals were quantified by densitometry. Mean densitometry data from independent experiments (one of which is shown here) were normalized to the result obtained in cells in the absence of bleomycin (control). (*D*) Sircol assay of soluble collagen content in the supernatants of bleomycin-treated cells from above. Values are mean ± SD ($n = 4$). *$P < 0.05$ versus nontreated control.

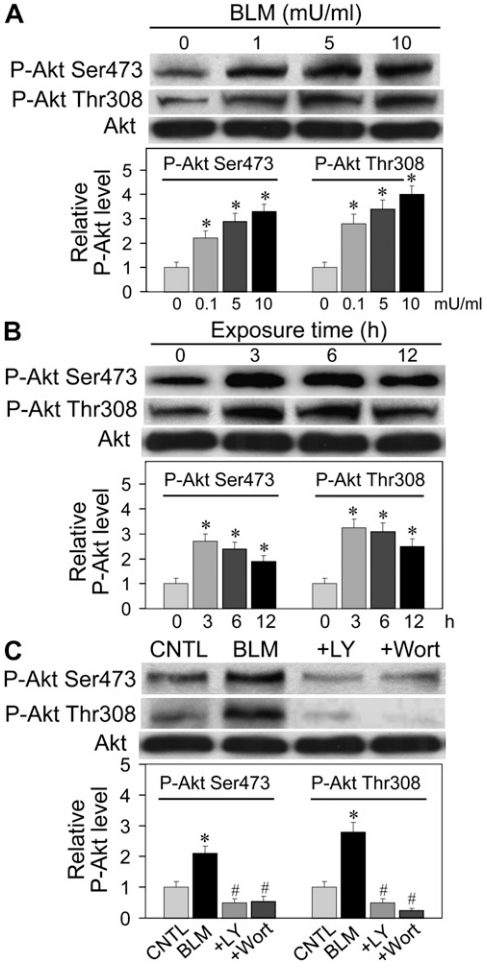

Figure 2. Induction of Akt phosphorylation by bleomycin and its inhibition by phosphatidylinositol-3-kinase (PI3K) inhibitors. (*A*) Dose effect of bleomycin on Akt phosphorylation. CRL-1490 cells were treated with various concentrations of bleomycin for 6 hours, after which they were washed with PBS and extracted with SDS sample buffer. The cell extracts were separated on 10% polyacrylamide-SDS gels, transferred, and probed with antibodies against phospho-Akt (Ser473 and Thr308) and Akt. (*B*) Time-dependent effect of bleomycin on Akt phosphorylation. Cells were treated with bleomycin (10 mU/ml) for various times and analyzed for phospho-specific and total Akt by immunoblotting. (*C*) Cells were either left untreated or pretreated with LY294002 (10 μM) or wortmannin (10 μM) for 1 hour, followed by bleomycin treatment (10 mU/ml) for 6 hours. Cell lysates were prepared and analyzed for phospho-Akt and total Akt. The immunoblot signals were quantified by densitometry. Values are mean ± SD ($n = 3$). $^*P < 0.05$ versus nontreated control, $^{\#}P < 0.05$ versus bleomycin-treated control.

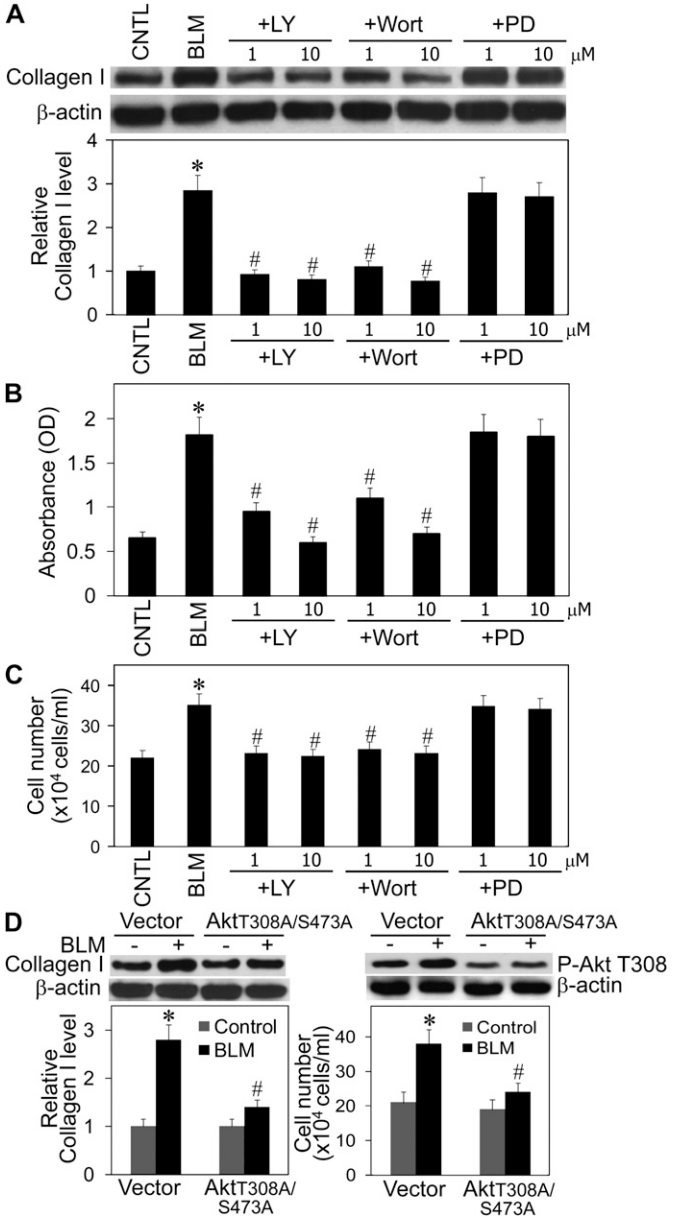

Figure 3. Effects of PI3K and mitogen-activated protein kinase/ERK kinase (MEK) inhibitors on bleomycin-induced collagen production and fibroblast cell growth. (*A*) CRL-1490 cells were either left untreated or pretreated for 1 hour with the indicated concentrations of LY294002, wortmannin, or PD98059, followed by bleomycin treatment (10 mU/ml) for 12 hours. Collagen protein expression was determined by Western blotting. The density of collagen bands was quantified and normalized against the nontreated control band. Plots show treatment effect on collagen type I expression. Similar results were observed with collagen type III. (*B*) Cell supernatants from above were analyzed for soluble collagen content by Sircol assay. (*C*) Cells were treated with the test agents as described above and assayed for cell growth after 24 hours. (*D*) Cells were stably transfected with Akt mutant (SRα-Akt T308A/S473A) plasmid or control plasmid as described in MATERIALS AND METHODS. Transfected cells were treated with bleomycin (10 mU/ml) for 12 hours and collagen expression, cell proliferation, and Akt phosphorylation were determined. Values are mean ± SD ($n = 3$). $^*P < 0.05$ versus nontreated control, $^{\#}P < 0.05$ versus bleomycin-treated control.

maximum growth response was observed at the treatment dose of 10 mU/ml. At higher doses, bleomycin caused apoptotic cell death as determined by ELISA-based DNA fragmentation assay (Figure 1B). Bleomycin also induced a dose-dependent effect on collagen protein expression. Figure 1C shows that collagen type I and III, two of the most abundant proteins of the ECM (35, 36), were induced by the bleomycin treatment. The induction of collagen by bleomycin was independent of its effect on cell growth, since collagen expression was determined on the basis of equal cellular protein per sample. Analysis of total collagen content in the cell supernatants of bleomycin-treated samples by Sircol assay similarly showed the dose-dependent effect of bleomycin on soluble collagen content (Figure 1D).

Together, these results indicate that bleomycin was able to directly induce fibroblast proliferation and collagen production in CRL-1490 cells.

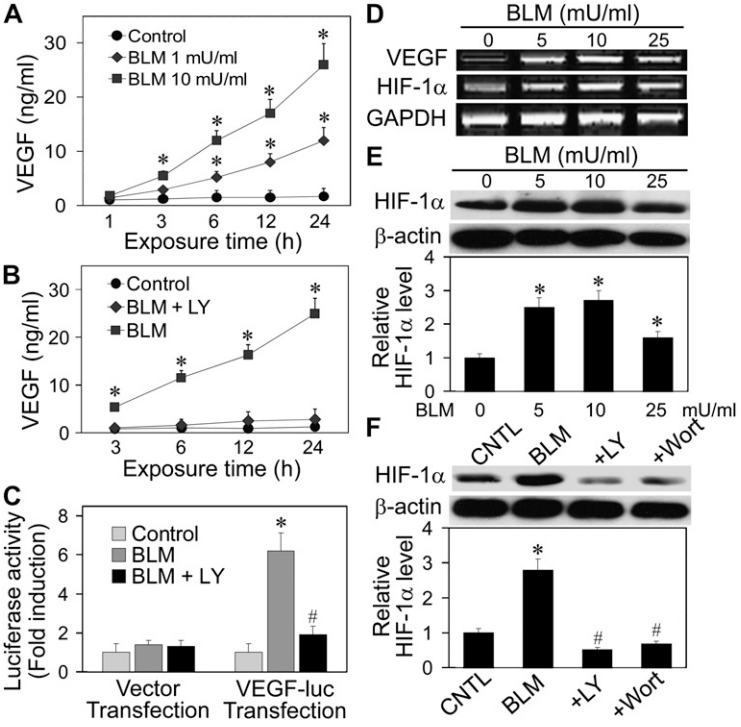

Figure 4. Effects of bleomycin and PI3K inhibitors on vascular endothelial growth factor (VEGF) and hypoxia-inducible factor-1α (HIF-1α) expression. (*A*) CRL-1490 cells were treated with the indicated concentrations of bleomycin and at various times after the treatment, cell supernatants were collected and analyzed for VEGF protein by ELISA. (*B*) Cells were treated with bleomycin (10 mU/ml) in the presence or absence of LY294002 (10 μM). At various times after the treatment, VEGF protein levels were determined as described. (*C*) Cells were transfected with 1 μg of either the VEGF reporter (VEGF-luc) or control plasmid and 10 ng of pRL-tk normalizing luciferase plasmid. Transfected cells were treated with bleomycin (10 mU/ml) in the presence or absence of LY294002 (10 μM), and analyzed for luciferase activity after 12 hours. (*D*) RT-PCR was done to quantify the expression of the indicated transcripts after treatment of the cells with various concentrations of bleomycin (0–25 mU/ml) for 12 hours. (*E*) Immunoblot analysis of HIF-1α protein expression after treatment of the cells with the indicated concentrations of bleomycin for 12 hours. Cell extracts were prepared, separated on 10% polyacrylamide-SDS gels, transferred, and probed with HIF-1α antibody. (*F*) Cells were either left untreated or pretreated with LY294002 (10 μM) or wortmannin (10 μM) for 1 hour, followed by bleomycin treatment (10 mU/ml) for 12 hours. Cell lysates were prepared and analyzed for HIF-1α. Blots were reprobed with β-actin antibody to confirm equal loading of the samples. The immunoblot signals were quantified by densitometry. Values are mean ± SD ($n = 3$). *$P < 0.05$ versus nontreated control, #$P < 0.05$ versus bleomycin-treated control.

Activation of Fibroblasts by Bleomycin is Dependent on PI3K/Akt

To determine whether PI3K/Akt plays a role in the fibrogenic effect of bleomycin, cells were treated with bleomycin in the presence or absence of PI3K inhibitors, LY294002 and wortmannin, and their effects on Akt expression and phosphorylation, as well as on fibroblast proliferation and collagen expression, were determined. Figures 2A and 2B show that bleomycin was able to induce Akt phosphorylation in a dose- and time-dependent manner, whereas it had no significant effect on total Akt protein level. The induction of Akt phosphorylation occurred at Thr308 and Ser473 positions, and this effect was inhibited by the PI3K inhibitors (Figure 2C), suggesting that bleomycin-induced Akt phosphorylation was through PI3K activation. The PI3K inhibitor LY294002 and wortmannin also inhibited bleomycin-induced fibroblast proliferation and collagen production (Figures 3A–3C). Furthermore, stable transfection of the cells with mutated Akt-T308A/S473A, which inhibited bleomycin-induced Akt phosphorylation (Figure 3D), caused a substantial decrease in the fibrogenic responses to bleomycin treatment as compared with control transfection (Figure 3D), supporting the role of PI3K and Akt phosphorylation in the fibrogenic effects of bleomycin. We also investigated whether mitogen-activated protein kinase/ERK kinase (MEK), which is an upstream activator of extracellular signal–regulated kinase (ERK), was involved in this induction. Cells were treated with bleomycin in the presence or absence of PD98059, a specific inhibitor of MEK, and its effects on cell proliferation and collagen production were similarly determined. Figures 3A–3C show that PD98059 had minimal effects on bleomycin-induced fibroblast proliferation and collagen expression. The result was confirmed by the observation that another ERK inhibitor, UO126, also had no significant effect on the fibroblast responses (data not shown). Together, these results suggest that PI3K/Akt, but not ERK, is involved in the growth and collagen inducing effects of bleomycin in lung fibroblasts.

Bleomycin Induces VEGF and HIF-1α

VEGF is a known target of PI3K/Akt signaling (34) and is upregulated in fibrotic lungs (12, 31, 32). Since Akt is activated by bleomycin (Figure 2), we tested whether VEGF could be induced by the bleomycin treatment through Akt signaling. Cells were treated with bleomycin and cell supernatants were collected and analyzed for VEGF at various times by ELISA. Figure 4A shows that VEGF protein levels were strongly induced by the bleomycin treatment in a dose- and time-dependent manner. At the concentrations of 1 and 10 mU/ml, bleomycin induced 12 ± 1 and 26 ± 3 ng/ml of VEGF, respectively, after a 24-hour treatment. The induction of VEGF by bleomycin was completely inhibited by the PI3K inhibitor LY294002 (Figure 4B), indicating that bleomycin-induced VEGF production was through the PI3K pathway. A similar effect was observed with wortmannin (data not shown). We also determined whether this induction is mediated through transcriptional activation of *VEGF*. Cells were transfected with a reporter plasmid carrying *VEGF* promoter (VEGF-luc) or a control plasmid. After transfection, the cells were treated with bleomycin in the presence or absence of LY294002 and their luciferase activity was determined by luminescence. Figure 4C shows that bleomycin induced a substantial increase in luciferase activity and that this induction was inhibited by the PI3K inhibitor. RT-PCR analysis of VEGF transcript further shows that bleomycin treatment increased VEGF mRNA levels in a dose-dependent manner (Figure 4D). Together, these results indicate that bleomycin induced transcriptional activation of VEGF through PI3K signaling.

Since HIF-1α is a known regulator of VEGF (28, 29), we tested whether this transcription factor is activated by the bleomycin treatment. Cells were treated with various concentrations of bleomycin (0–25 mU/ml) and HIF-1α expression was determined by RT-PCR and Western blot analysis. Figures 4D and 4E show that HIF-1α transcript and protein levels were induced by the bleomycin treatment with a maximal dose response observed at 10 mU/ml. Figure 4F further shows that

the induction of HIF-1α by bleomycin was inhibited by the PI3K inhibitors LY294002 and wortmannin, supporting the role of PI3K/Akt in bleomycin-induced HIF-1α activation.

HIF-1α Regulates Bleomycin-Induced VEGF Production

To determine the potential regulation of VEGF by HIF-1α in bleomycin-treated cells, cells were transfected with HIF-1α shRNA (shHIF) viral particles or control shRNA (shCON) particles, and their effects on bleomycin-induced VEGF production was determined. Western blot analysis of HIF-1α in the transfected cells shows a substantial reduction in HIF-1α expression in the shHIF-transfected cells as compared with shCON-transfected cells (Figure 5A). The shHIF-transfected cells also produced less VEGF than the control transfected cells in response to bleomycin treatment (Figure 5B). We also tested the effect of HIF-1α knockdown on collagen expression and fibroblast proliferation. Figures 5C and 5D show that the shHIF-transfected cells expressed significantly lower level of collagen and were less responsive to cell growth induced by bleomycin as compared with control transfected cells. Together, these results indicate the role of HIF-1α as a positive regulator of VEGF and fibrogenic signaling in bleomycin-treated lung fibroblasts.

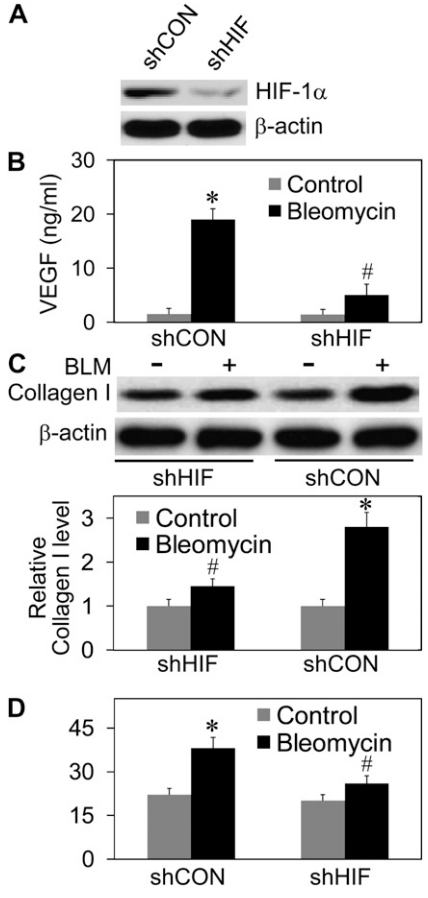

Figure 5. Effects of HIF-1α knockdown on bleomycin-induced VEGF secretion, fibroblast proliferation, and collagen expression. CRL-1490 cells were transfected with HIF-1α shRNA (shHIF) viral particles or control shRNA (shCON) particles as described in MATERIALS AND METHODS. (*A*) Thirty-six hours after the transfection, cells were analyzed for HIF-1α expression by Western blotting. (*B* and *C*) Transfected cells were treated with bleomycin (10 mU/ml) for 12 hours and analyzed for VEGF secretion by ELISA and collagen expression by Western blotting. (*D*) Cell growth determined at 24 hours after bleomycin treatment (10 mU/ml). Values are mean ± SD ($n = 3$). $^{*}P < 0.05$ versus nontreated control, $^{\#}P < 0.05$ versus shCON-treated control.

VEGF Induces Fibroblast Proliferation and Collagen Expression

Since VEGF is a key effector molecule of the PI3K/Akt/HIF-1α signaling pathway, we tested whether VEGF could be a key mediator of the fibrogenic effect of bleomycin. First, cells were treated with VEGF at the concentrations induced by bleomycin (10–25 ng/ml), and cell proliferation and collagen expression of lung fibroblasts were determined. Figures 6A and 6B show that VEGF was able to induce collagen expression and fibroblast proliferation in a dose-dependent manner; however, such inductions were less pronounced than those observed with bleomycin. Second, cells were treated with bleomycin in the presence of neutralizing anti-VEGF antibody or control antibody, and their effects on fibroblast proliferation and collagen expression were determined. Figures 6C and 6D show that as compared with control antibody treatment, the neutralizing antibody treatment significantly inhibited the growth- and collagen-inducing effects of bleomycin. However, such inhibition was incomplete, and increasing the concentration of the neutralizing antibody beyond the indicated concentration (100 ng/ml) did not result in further inhibition. These results suggest that although VEGF could be a key mediator of the fibrogenic effect of bleomycin, other mediators induced by PI3K/Akt or other mechanisms of fibroblast activation are also involved.

Requirement of ROS for Bleomycin-Induced PI3K/Akt Activation

To determine whether the activation of PI3K/Akt by bleomycin is mediated by ROS, which has not been demonstrated, we

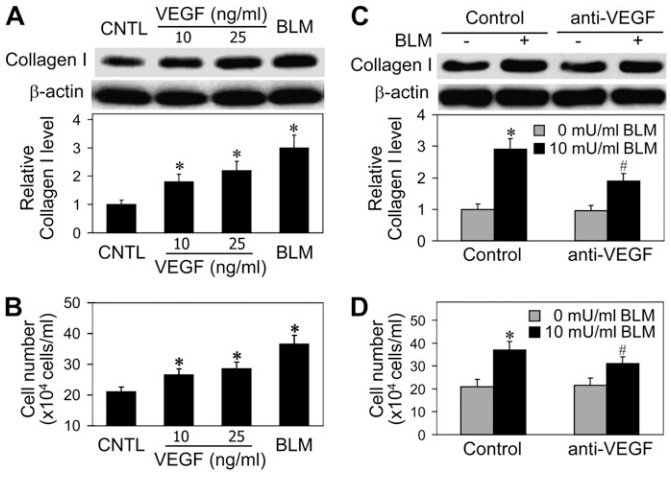

Figure 6. Effects of VEGF on collagen expression and fibroblast proliferation. (*A*) CRL-1490 cells were treated with recombinant VEGF (10 and 25 ng/ml) for 12 hours and analyzed for collagen expression by Western blotting. Bleomycin (10 mU/ml) was used as a positive control. Densitometry was performed to determine the relative levels of collagen expression after reprobing with β-actin antibody. (*B*) Cells were similarly treated with VEGF and bleomycin, and analyzed for cell growth after 24 hours. (*C* and *D*) Cells were treated with bleomycin (10 mU/ml) in the presence of neutralizing anti-VEGF or control antibody (100 ng/ml), and collagen expression and cell growth were determined after 12 hours and 24 hours, respectively. Values are mean ± SD ($n = 4$). $^{*}P < 0.05$ versus nontreated control, $^{\#}P < 0.05$ less than control antibody treatment with bleomycin but greater than non–bleomycin-treated control.

studied the effects of bleomycin on cellular ROS generation and PI3K/Akt activation. Cells were treated with various concentrations of bleomycin, and ROS generation was determined by fluorometry using hydroethidine (DHE) and dichlorofluorescein diacetate (DCF-DA) as oxidative probes. Figure 7A shows that bleomycin induced a dose-dependent increase in cellular DHE and DCF fluorescence intensities, indicative of superoxide and peroxide formation, respectively. The potential role of ROS in bleomycin-induced Akt activation was further examined by evaluating the effect of MnTBAP (a superoxide dismutase mimetic and $O_2^{-\cdot}$ scavenger) and catalase (H_2O_2 scavenger) on bleomycin-induced Akt phosphorylation. Figure 7B shows that both MnTBAP and catalase completely inhibited bleomycin-induced Akt phosphorylation. Total Akt levels were relatively unaffected by these treatments. The ability of the antioxidants to inhibit Akt activation by bleomycin indicates the role of ROS in this process. Bleomycin-induced lung fibrosis has been reported to be associated with increased ROS production (37, 38). To test whether ROS might mediate the fibrogenic effect of bleomycin through PI3K/Akt→HIF-1α→VEGF signaling, we evaluated the effect of antioxidants on bleomycin-induced HIF-1α and VEGF activation. Figures 7C and 7D show that the antioxidants MnTBAP and catalase strongly inhibited HIF-1α and VEGF expression induced by bleomycin. MnTBAP and catalase treatment alone had minimal effects on cytokine expression and Akt phosphorylation in unstimulated cells (data not shown). These results support the role of ROS in fibrogenic signaling induced by bleomycin.

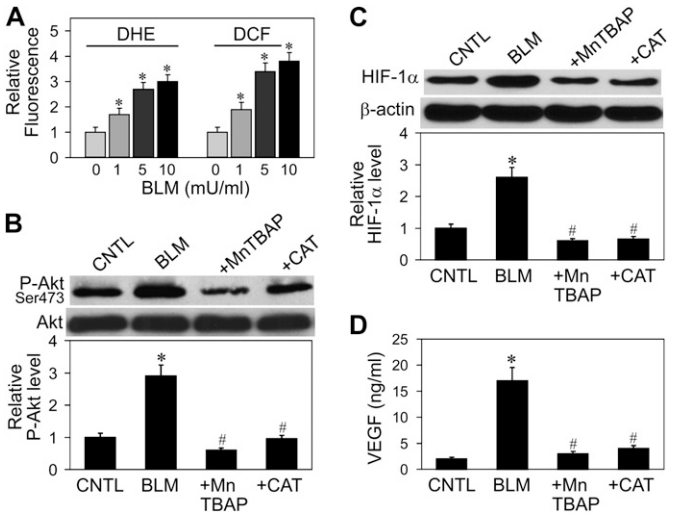

Figure 7. Induction of reactive oxygen species (ROS) generation by bleomycin and its effects on Akt, HIF-1α, and VEGF expression. (*A*) CRL-1490 cells were treated with various concentrations of bleomycin (0–10 mU/ml) and analyzed for ROS production by measuring DHE and DCF fluorescence intensities. Plots show relative fluorescence intensity over nontreated control at the peak response time of 3 hours after treatment. (*B*) Cells were pretreated for 1 hour with MnTBAP (100 μM) or catalase (1,000 U/ml), and then treated with bleomycin (10 mU/ml) for 6 hours and analyzed for Akt phosphorylation and expression by Western blotting. (*C*) Cells were pretreated for 1 hour with MnTBAP (100 μM) or catalase (1,000 U/ml), and then treated with bleomycin (10 mU/ml) for 12 hours and analyzed for HIF-1α expression by Western blotting. Blots were reprobed with β-actin antibody to confirm equal loading of the samples. The immunoblot signals were quantified by densitometry. (*D*) Cells were pretreated for 1 hour with MnTBAP (100 μM) or catalase (1,000 U/ml), and then treated with bleomycin (10 mU/ml) for 12 hours and analyzed for VEGF protein levels by ELISA. Values are mean ± SD ($n = 3$). *$P < 0.05$ versus nontreated control, #$P < 0.05$ versus bleomycin-treated control.

Involvement of ROS in Bleomycin-Induced Fibroblast Proliferation and Collagen Production

Having demonstrated the role of ROS in bleomycin-induced PI3K/Akt activation and HIF-1α and VEGF expression, we next determined the effects of ROS on bleomycin-induced fibroblast proliferation and collagen production. Cells were treated with bleomycin in the presence or absence of MnTBAP and catalase, and their effects on fibroblast proliferation and collagen production were determined. Figures 8A–8C show that MnTBAP and catalase strongly inhibited the proliferative and collagen-inducting effects of bleomycin, whereas MnTBAP and catalase control treatment had minimal effects (data not shown). Together, these results support the role of ROS as a key regulator of fibrogenesis induced by bleomycin through PI3K/Akt activation.

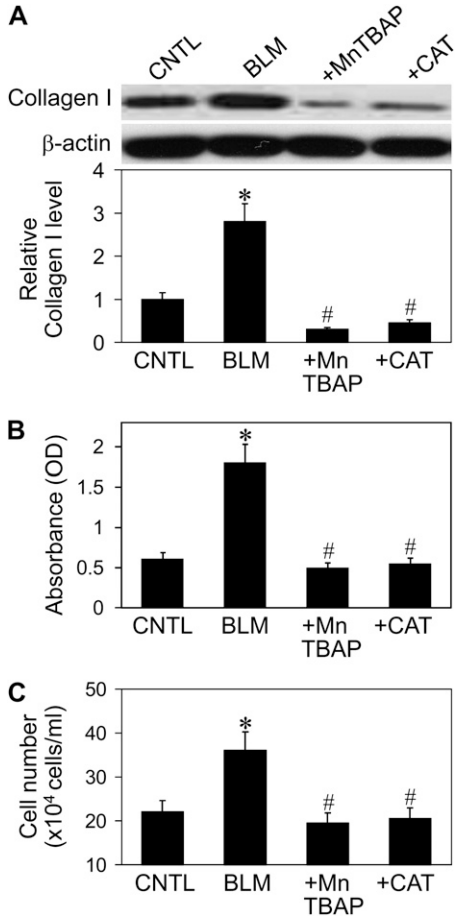

Figure 8. Effects of ROS on bleomycin-induced collagen production and fibroblast proliferation. (*A*) CRL-1490 cells were pretreated for 1 hour with MnTBAP (100 μM) or catalase (1,000 U/ml), and then treated with bleomycin (10 mU/ml) for 12 hours and analyzed for collagen by Western blotting. Blots were reprobed with β-actin antibody to confirm equal loading of the samples. The immunoblot signals were quantified by densitometry. (*B*) Cell supernatants from above were analyzed for soluble collagen content by Sircol assay. (*C*) Cells were pretreated for 1 hour with MnTBAP (100 μM) or catalase (1,000 U/ml), and then treated with bleomycin (10 mU/ml) for 24 hours and analyzed for cell growth. Values are mean ± SD ($n = 4$). *$P < 0.05$ versus nontreated control, #$P < 0.05$ versus bleomycin-treated control.

DISCUSSION

The role of PI3K/Akt in cell survival and angiogenesis is well established, but its role in fibrogenesis is not well understood. In this study, we demonstrated that PI3K/Akt plays an important role in fibrogenesis of human lung fibroblasts induced by bleomycin by up-regulating cell growth and collagen expression. The effect of bleomycin on cell growth is dose dependent. At low doses (0.1–10 mU/ml) bleomycin promoted cell growth, whereas at higher doses it induced apoptotic cell death (Figure 1). This latter effect of bleomycin was previously reported by Yen and coworkers (39) in human lung fibroblast W138 cells. In primary lung fibroblasts isolated from rats, Koslowski and colleagues (40) showed that bleomycin induced terminal differentiation of the cells at the same dose range that was shown in this study to stimulate cell growth. This discrepancy may be attributed to the lack of proliferative capacity of the isolated lung cells *in vitro* undergoing terminal differentiation. However, both studies demonstrated the collagen-inducing effect of bleomycin at the same dose range, which is consistent with a previous report by Yamamoto and coworkers (41) in skin fibroblasts.

Bleomycin induced Akt phosphorylation at ser473 and thr308 positions through PI3K activation, which is required for the induction of fibroblast proliferation and collagen expression (Figures 2 and 3). Previous studies have shown that PI3K is involved in the activation of Akt under various physiologic and pathologic conditions (14, 39, 42); however, PI3K-independent mechanisms of Akt activation have also been reported (43, 44). In this study, we found that PI3K is an important upstream regulator of bleomycin-induced Akt activation, and that ERK pathway plays a minor role in this process (Figure 3). The results of this study also demonstrated that the activation of PI3K/Akt by bleomycin requires ROS generation, and that this ROS induction plays a crucial role in the regulation of fibroblast proliferation and collagen expression induced by bleomycin. ROS have been shown to play a role in various cellular processes, but its role in fibrogenesis and the regulatory mechanisms are unclear. We found that ROS was induced by the fibrogenic agent bleomycin and that inhibition of ROS by the antioxidant enzyme catalase and MnTBAP strongly inhibited the growth- and collagen-inducing effects of bleomycin (Figure 8). Likewise, both MnTBAP and catalase inhibited the activation of Akt by bleomycin (Figure 7), supporting the role of Akt and its regulation by ROS in the fibrogenic process. The requirement of ROS in bleomycin-induced Akt activation and fibrogenesis has not been reported, and our results provide evidence supporting its role and identify key ROS involved (i.e., superoxide anion and hydrogen peroxide).

Several mechanisms of bleomycin-induced fibrosis have been proposed, including epithelial cell injury, basement membrane disruption, ECM remodeling, and angiogenesis. After injury, the epithelium initiates a wound healing process to restore the integrity of its barrier. This process is facilitated by connective tissue cells, in particular fibroblasts, which produce ECM that promotes epithelial cell migration and re-epithelialization (45). Uncontrolled or excessive production of ECM by fibroblasts is widely believed to be a key contributing factor in the development of lung fibrosis. Activation of fibroblast proliferation and accumulation of ECM during the repair process necessitate neovascularization, and increasing evidence supports its role in fibrogenesis (35, 45, 46). The angiogenic process is known to involve an intricate cytokine network that activates and mediates interactions between multiple cell types. A key mediator of angiogenesis is VEGF, which is overexpressed in fibrotic lungs (12, 30) and is known to be activated by the transcription factor HIF-1α (28, 29). Our results show that bleomycin induced HIF-1α gene and protein expression in a dose-dependent manner (Figures 4D and 4E). This effect of bleomycin was inhibited by PI3K inhibitors (Figure 4F), indicating that bleomycin induces HIF-1α activation through the PI3K/Akt pathway. Consistent with previous reports showing the regulatory role of HIF-1α on VEGF expression (26, 27, 47), we found that VEGF gene and protein expression was also up-regulated by the bleomycin treatment and that this effect can be inhibited by the PI3K inhibitor LY294002 (Figures 4A–4C). Therefore, in response to bleomycin, PI3K/Akt may be the major signaling pathway regulating VEGF via HIF-1α activation, which is supported by our experimental data (Figure 5). Furthermore, ROS scavengers, MnTBAP and catalase, also inhibited bleomycin-induced HIF-1α and VEGF expression (Figures 7C and 7D). Since ROS also regulates PI3K/Akt signaling in response to bleomycin treatment, it is likely that ROS may serve as an upstream regulator of the fibrogenic signaling via PI3K/Akt → HIF-1α → VEGF pathway.

Our results also demonstrated that VEGF exerted a direct stimulating effect on lung fibroblasts, inducing their proliferation and collagen expression (Figures 6A and 6B). Although VEGF was induced by bleomycin (Figure 4A) and its neutralization by anti-VEGF antibody significantly inhibited the fibrogenic effects of bleomycin (Figures 6C and 6D), VEGF alone could not account for the total fibrogenic effects of bleomycin. These results indicate that other fibrogenic mediators induced by bleomycin or other mechanisms of fibrogenic induction are also involved. However, the observation that bleomycin-induced fibroblast activation was completely inhibited by PI3K inhibitors (Figure 3) suggests that PI3K/Akt-mediated fibrogenic factors are critically involved. Several growth factors under the regulation of PI3K/Akt, including platelet-derived growth factor (PDGF) and transforming growth factor-β (TGF-β), have been reported (48, 49). These growth factors along with several others, including basic fibroblast growth factor, ephrin-B2, angiopoietins, and VEGF, have also been reported to regulate PI3K/Akt (50) and have been implicated in the pathogenesis of lung fibrosis (11, 12, 51). Furthermore, PDGF and TGF-β are known to be indirect angiogenic mediators by promoting angiogenesis through PI3K/Akt signaling (52, 53). Thus, PI3K/Akt may regulate fibrogenesis through multiple mechanisms that involve various cytokines and growth factors.

In summary, our data provide evidence that bleomycin induces a direct fibrogenic effect on lung fibroblasts by up-regulating collagen expression and cell proliferation through PI3K/Akt signaling. Bleomycin also induces HIF-1α and VEGF expression, which contributes, at least in part, to the fibrogenic effect of bleomycin. Such induction requires ROS generation, particularly superoxide anion and hydrogen peroxide. This finding adds fibrogenesis to the growing lists of cellular events that are regulated by ROS-mediated PI3K/Akt signaling. Since fibroblast proliferation and collagen accumulation are key characteristics of lung fibrosis, understanding its regulatory mechanisms could aid in the development of more effective therapies for the disease.

Conflict of Interest Statement: None of the authors has a financial relationship with a commercial entity that has an interest in the subject of this manuscript.

References

1. Crouch E. Pathobiology of pulmonary fibrosis. *Am J Physiol* 1990;259: L159–L184.
2. Thannickal VJ, Toews GB, White ES, Lynch JP III, Martinez FJ. Mechanisms of pulmonary fibrosis. *Annu Rev Med* 2004;55:395–417.
3. Raghu G, Freudenberger TD, Yang S, Curtis JR, Spada C, Hayes J, Sillery JK, Pope CE II, Pellegrini CA. High prevalence of abnormal acid gastro-oesophageal reflux in idiopathic pulmonary fibrosis. *Eur Respir J* 2006;27:136–142.

4. Coultas DB, Zumwalt RE, Black WC, Sobonya RE. The epidemiology of interstitial lung diseases. *Am J Respir Crit Care Med* 1994;150: 967–972.
5. Ask K, Bonniaud P, Maass K, Eickelberg O, Margetts PJ, Warburton D, Groffen J, Gauldie J, Kolb M. Progressive pulmonary fibrosis is mediated by TGF-β isoform 1 but not TGF-β3. *Int J Biochem Cell Biol* 2008;40:484–495.
6. Gharaee-Kermani M, Gyetko MR, Hu B, Phan SH. New insights into the pathogenesis and treatment of idiopathic pulmonary fibrosis: a potential role for stem cells in the lung parenchyma and implications for therapy. *Pharm Res* 2007;24:819–841.
7. Katzenstein AL, Myers JL. Idiopathic pulmonary fibrosis: clinical relevance of pathologic classification. *Am J Respir Crit Care Med* 1998;157:1301–1315.
8. Kuhn C, McDonald JA. The roles of the myofibroblast in idiopathic pulmonary fibrosis: ultrastructural and immunohistochemical features of sites of active extracellular matrix synthesis. *Am J Pathol* 1991;138: 1257–1265.
9. Flaherty KR, Toews GB, Lynch JP III, Kazerooni EA, Gross BH, Strawderman RL, Hariharan K, Flint A, Martinez FJ. Steroids in idiopathic pulmonary fibrosis: a prospective assessment of adverse reactions, response to therapy, and survival. *Am J Med* 2001;110:278–282.
10. King TE Jr, Schwarz MI, Brown K, Tooze JA, Colby TV, Waldron JA Jr, Flint A, Thurlbeck W, Cherniack RM. Idiopathic pulmonary fibrosis: relationship between histopathologic features and mortality. *Am J Respir Crit Care Med* 2001;164:1025–1032.
11. Nobel JJ, Norman GK. Emerging information management technologies and the future of disease management. *Dis Manag* 2003;6:219–231.
12. Steurer M, Zoller H, Augustin F, Fong D, Heiss S, Strasser-Weippl K, Gastl G, Tzankov A. Increased angiogenesis in chronic idiopathic myelofibrosis: vascular endothelial growth factor as a prominent angiogenic factor. *Hum Pathol* 2007;38:1057–1064.
13. Clark RA, Mason RJ, Folkvord JM, McDonald JA. Fibronectin mediates adherence of rat alveolar type II epithelial cells via the fibroblastic cell-attachment domain. *J Clin Invest* 1986;77:1831–1840.
14. Cantley LC. The phosphoinositide 3-kinase pathway. *Science* 2002;296: 1655–1657.
15. Roymans D, Grobben B, Claes P, Slegers H. Protein tyrosine kinase-dependent regulation of adenylate cyclase and phosphatidylinositol 3-kinase activates the expression of glial fibrillary acidic protein upon induction of differentiation in rat c6 glioma. *Cell Biol Int* 2001;25:467–474.
16. Luo J, Manning BD, Cantley LC. Targeting the PI3K-Akt pathway in human cancer: rationale and promise. *Cancer Cell* 2003;4:257–262.
17. Sable CL, Filippa N, Filloux C, Hemmings BA, Van Obberghen E. Involvement of the pleckstrin homology domain in the insulin-stimulated activation of protein kinase B. *J Biol Chem* 1998;273: 29600–29606.
18. Jiang BH, Jiang G, Zheng JZ, Lu Z, Hunter T, Vogt PK. Phosphatidylinositol 3-kinase signaling controls levels of hypoxia-inducible factor 1. *Cell Growth Differ* 2001;12:363–369.
19. Minet E, Arnould T, Michel G, Roland I, Mottet D, Raes M, Remacle J, Michiels C. ERK activation upon hypoxia: involvement in HIF-1 activation. *FEBS Lett* 2001;468:53–58.
20. Richard DE, Berra E, Gothie E, Roux D, Pouyssegur J. p42/p44 mitogen-activated protein kinases phosphorylate hypoxia-inducible factor 1alpha (HIF-1α) and enhance the transcriptional activity of HIF-1. *J Biol Chem* 1999;274:32631–32637.
21. Zhong H, Chiles K, Feldser D, Laughner E, Hanrahan C, Georgescu MM, Simons JW, Semenza GL. Modulation of hypoxia-inducible factor 1α expression by the epidermal growth factor/phosphatidylinositol 3-kinase/PTEN/AKT/FRAP pathway in human prostate cancer cells: implications for tumor angiogenesis and therapeutics. *Cancer Res* 2000;60:1541–1545.
22. Gao N, Ding M, Zheng JZ, Zhang Z, Leonard SS, Liu KJ, Shi X, Jiang BH. Vanadate-induced expression of hypoxia-inducible factor 1α and vascular endothelial growth factor through phosphatidylinositol 3-kinase/Akt pathway and reactive oxygen species. *J Biol Chem* 2002; 277:31963–31971.
23. Hellwig-Burgel T, Stiehl DP, Katschinski DM, Marxsen J, Kreft B, Jelkmann W. VEGF production by primary human renal proximal tubular cells: requirement of HIF-1, PI3-kinase and MAPKK-1 signaling. *Cell Physiol Biochem* 2005;15:99–108.
24. Tacchini L, De Ponti C, Matteucci E, Follis R, Desiderio MA. Hepatocyte growth factor-activated NF-κB regulates HIF-1 activity and ODC expression, implicated in survival, differently in different carcinoma cell lines. *Carcinogenesis* 2004;25:2089–2100.
25. Hoffman EC, Reyes H, Chu FF, Sander F, Conley LH, Brooks BA, Hankinson O. Cloning of a factor required for activity of the Ah (dioxin) receptor. *Science* 1991;252:954–958.
26. Wang GL, Jiang BH, Rue EA, Semenza GL. Hypoxia-inducible factor 1 is a basic-helix-loop-helix-PAS heterodimer regulated by cellular O_2 tension. *Proc Natl Acad Sci USA* 1995;92:5510–5514.
27. Jiang BH, Semenza GL, Bauer C, Marti HH. Hypoxia-inducible factor 1 levels vary exponentially over a physiologically relevant range of O_2 tension. *Am J Physiol* 1996;271:C1172–C1180.
28. Forsythe JA, Jiang BH, Iyer NV, Agani F, Leung SW, Koos RD, Semenza GL. Activation of vascular endothelial growth factor gene transcription by hypoxia-inducible factor 1. *Mol Cell Biol* 1996;16: 4604–4613.
29. Liu Y, Cox SR, Morita T, Kourembanas S. Hypoxia regulates vascular endothelial growth factor gene expression in endothelial cells: identification of a 5′ enhancer. *Circ Res* 1995;77:638–643.
30. Carmeliet P. Mechanisms of angiogenesis and arteriogenesis. *Nat Med* 2000;6:389–395.
31. Meyer KC, Cardoni A, Xiang ZZ. Vascular endothelial growth factor in bronchoalveolar lavage from normal subjects and patients with diffuse parenchymal lung disease. *J Lab Clin Med* 2000;135:332–338.
32. Fehrenbach H, Kasper M, Haase M, Schuh D, Muller M. Differential immunolocalization of VEGF in rat and human adult lung, and in experimental rat lung fibrosis: light, fluorescence, and electron microscopy. *Anat Rec* 1999;254:61–73.
33. Gao N, Shen L, Zhang Z, Leonard SS, He H, Zhang XG, Shi X, Jiang BH. Arsenite induces HIF-1α and VEGF through PI3K, Akt and reactive oxygen species in DU145 human prostate carcinoma cells. *Mol Cell Biochem* 2004;255:33–45.
34. Jiang BH, Zheng JZ, Aoki M, Vogt PK. Phosphatidylinositol 3-kinase signaling mediates angiogenesis and expression of vascular endothelial growth factor in endothelial cells. *Proc Natl Acad Sci USA* 2000; 97:1749–1753.
35. Brinckerhoff CE, Matrisian LM. Matrix metalloproteinases: a tail of a frog that became a prince. *Nat Rev Mol Cell Biol* 2002;3:207–214.
36. Pardo A, Selman M. MMP-1: the elder of the family. *Int J Biochem Cell Biol* 2005;37:283–288.
37. Inghilleri S, Morbini P, Oggionni T, Barni S, Fenoglio C. In situ assessment of oxidant and nitrogenic stress in bleomycin pulmonary fibrosis. *Histochem Cell Biol* 2006;125:661–669.
38. Quinlan T, Spivack S, Mossman BT. Regulation of antioxidant enzymes in lung after oxidant injury. *Environ Health Perspect* 1994;102:79–87.
39. Yen SC, Chang HM, Majima HJ, Chen FY, Li SH. Levels of reactive oxygen species and primary antioxidant enzymes in WI38 versus transformed WI38 cells following bleomcyin treatment. *Free Radic Biol Med* 2005;38:950–959.
40. Koslowski R, Morgner J, Siedel D, Knoch KP, Kasper M. Postmitotic differentiation of rat lung fibroblasts: induction by bleomycin and effect on prolyl 4-hydroxylase. *Exp Toxicol Pathol* 2004;55:481–487.
41. Yamamoto T, Eckes B, Krieg T. Bleomycin increases steady-state levels of type I collagen, fibronectin and decorin mRNAs in human skin fibroblasts. *Arch Dermatol Res* 2000;292:556–561.
42. Corvera S, Czech MP. Direct targets of phosphoinositide 3-kinase products in membrane traffic and signal transduction. *Trends Cell Biol* 1998;8:442–446.
43. Franke TF, Kaplan DR, Cantley LC. PI3K: downstream AKTion blocks apoptosis. *Cell* 1997;88:435–437.
44. Moule SK, Welsh GI, Edgell NJ, Foulstone EJ, Proud CG, Denton RM. Regulation of protein kinase B and glycogen synthase kinase-3 by insulin and β-adrenergic agonists in rat epididymal fat cells: activation of protein kinase B by wortmannin-sensitive and -insensitive mechanisms. *J Biol Chem* 1997;272:7713–7719.
45. Selman M, King TE, Pardo A. Idiopathic pulmonary fibrosis: prevailing and evolving hypotheses about its pathogenesis and implications for therapy. *Ann Intern Med* 2001;134:136–151.
46. Selman M, Montano M, Ramos C, Chapela R. Concentration, biosynthesis and degradation of collagen in idiopathic pulmonary fibrosis. *Thorax* 1986;41:355–359.
47. Gong P, Hu B, Stewart D, Ellerbe M, Figueroa YG, Blank V, Beckman BS, Alam J. Cobalt induces heme oxygenase-1 expression by a hypoxia-

inducible factor-independent mechanism in Chinese hamster ovary cells: regulation by Nrf2 and MafG transcription factors. *J Biol Chem* 2001;276: 27018–27025.
48. Bakin AV, Tomlinson AK, Bhowmick NA, Moses HL, Arteaga CL. Phosphatidylinositol 3-kinase function is required for transforming growth factor β-mediated epithelial to mesenchymal transition and cell migration. *J Biol Chem* 2000;275:36803–36810.
49. Romashkova JA, Makarov SS. NF-κB is a target of AKT in anti-apoptotic PDGF signalling. *Nature* 1999;401:86–90.
50. Hamada K, Sasaki T, Koni PA, Natsui M, Kishimoto H, Sasaki J, Yajima N, Horie Y, Hasegawa G, Naito M, *et al.* The PTEN/PI3K pathway governs normal vascular development and tumor angiogenesis. *Genes Dev* 2005;19:2054–2065.
51. Arora B, Mesa R, Tefferi A. Angiogenesis and anti-angiogenic therapy in myelofibrosis with myeloid metaplasia. *Leuk Lymphoma* 2004;45: 2373–2386.
52. Yang EY, Moses HL. Transforming growth factor β1-induced changes in cell migration, proliferation, and angiogenesis in the chicken chorioallantoic membrane. *J Cell Biol* 1990;111:731–741.
53. Cao Y, Cao R, Hedlund EM. Regulation of tumor angiogenesis and metastasis by FGF and PDGF signaling pathways. *J Mol Med* 2008;86: 785–789.